International Journal of Non–Linear Mechanics 159 (2024) 104567

Contents lists available at ScienceDirect

International Journal of Non-Linear Mechanics

journal homepage: www.elsevier.com/locate/nlm

Nonlinear vibrations of beams with fractional derivative elements crossed by moving loads

Alba Sofi

Department of Architecture and Territory and Inter-University Centre of Theoretical and Experimental Dynamics, University "Mediterranea" of Reggio Calabria, Via dell'Università 25, 89124, Reggio, Calabria, Italy

ARTICLE INFO

Keywords:
Nonlinear beam
Fractional differential equations
Step-by-step integration
Pseudo-force

ABSTRACT

This paper addresses the evaluation of the time-domain response of nonlinear beams endowed with a fractional derivative element crossed by moving loads. Nonlinearities originate from the assumption of moderately large displacements of the beam. Following a Galerkin-type solution procedure, beam transversal displacement is represented in terms of the linear modes of vibration and time-dependent generalized coordinates. A novel step-by-step integration scheme, labeled *improved pseudo-force method* (*IPFM*), is developed for the numerical solution of the set of coupled nonlinear fractional differential equations governing the time-dependent generalized coordinates. The proposed procedure stems from the extension of a recently developed step-by-step scheme for the dynamic analysis of fractional single-degree-of-freedom systems. The *IPFM* involves the following main steps: *i*) to apply the Grünwald–Letnikov approximation of the fractional derivative; *ii*) to treat terms depending on the unknown values of the response as *pseudo-forces*; *iii*) to handle nonlinearities by performing iterations at each time step.

Numerical results are presented to assess the accuracy of the *IPFM* as well as to investigate the influence of the fractional derivative order and coefficient on nonlinear beam vibrations under moving loads.

1. Introduction

Nowadays, fractional calculus [1,2] is successfully applied to model several phenomena in material science and engineering, such as viscoelasticity, diffusion in porous media, heat conduction, wave propagation, etc. [3–6]. In their pioneering studies on fractional viscoelasticity, Nutting [7] and Gemant [8] observed that experimental data from relaxation tests on viscoelastic materials, such as rubber, bitumen, polymers, etc., are well fitted by a power-law function [9]. Since the first attempt of Bagley and Torvik [10–12] to provide a theoretical basis for fractional viscoelasticity, fractional-derivative modelling of the constitutive behaviour of viscoelastic materials has become a well-established tool in continuum and structural mechanics. The power-law kernels of fractional operators are capable of capturing both relaxation and creep behaviors just by means of two parameters thus overcoming the limitations of the classical Maxwell and Kelvin–Voigt rheological models of viscoelasticity. Comprehensive reviews on the applications of fractional calculus to dynamic problems of mechanics of solids were provided by Rossikhin and Shitikova [13,14] and Shitikova [15].

An application of prominent engineering interest lies in the use of fractional calculus to model the viscoelastic behaviour of continuous elastic beams. Starting from the local fractional viscoelastic relationship between axial stress and axial strain, Di Paola et al. [16] addressed the response evaluation of viscoelastic Euler–Bernoulli beams under quasi-static and dynamic loads. Taking advantage of the Mellin transform method, Pirrotta et al. [17] determined the response of fractional Timoshenko beams in the time-domain. Both the procedures proposed in Refs. [16,17] avoid resorting to the commonly used Laplace Transform approach (see e.g., Ref. [18]) which is unable to unveil the physical implications of fractional hereditary behaviour.

Nonlinear vibrations of viscoelastic beams have also been analyzed by using different fractional viscoelastic models. Assuming a fractional Zener rheological model, Lewandowski and Wielentejczyk [19] studied nonlinear steady-state vibrations of viscoelastic beams under harmonic excitation by combining the harmonic balance and finite element methods to obtain the amplitude equations which are then solved by a continuation method. More recently, Lewandowski [20] applied an exponential version of the harmonic balance method to analyze nonlinear steady-state vibrations of beams made of the fractional Zener material. Zhang et al. [21] investigated the nonlinear dynamic response of a simply supported viscoelastic beam subjected to transverse harmonic excitations assuming a fractional Kelvin constitutive model.

E-mail address: alba.sofi@unirc.it.

https://doi.org/10.1016/j.ijnonlinmec.2023.104567
Received 27 September 2023; Accepted 12 October 2023
Available online 20 October 2023

Liakos et al. [22] derived implicit analytical solutions for the nonlinear fractional partial differential equation governing the dynamics of a deterministically excited nonlinear Euler-Bernoulli beam resting on a viscoelastic foundation. Javadi and Rahmanian [23] analyzed the nonlinear vibrations of fractional Kelvin–Voigt viscoelastic beams on a nonlinear elastic foundation under harmonic excitation by applying the Galerkin technique and the method of multiple scales.

The analysis of linear [24,25] and nonlinear beams [26–28] with fractional derivative elements subjected to stochastic excitations has also been addressed over the last decades. By combining normal mode and Laplace transform techniques, Agrawal [24] derived analytical solutions for the stochastic response of fractionally damped continuous beams. Liakos et al. [25] provided implicit analytical solutions for the linear stochastic partial differential equation with fractional derivative terms governing the dynamics of a stochastically excited Euler–Bernoulli beam resting on a viscoelastic foundation. Spanos and Malara [26] analyzed nonlinear random vibrations of a beam comprising a fractional derivative element by developing a statistical linearization approach based on an appropriate iterative representation of the stochastic response spectrum, which involves the linear modes of vibration of the beam. Moderately large vibrations of beams and plates endowed with fractional derivative elements excited by combinations of harmonic and random loads were analyzed in Ref. [27] by representing the system response as the superposition of the linear modes of vibration. Response statistics were estimated by employing the statistical linearization technique in conjunction with the harmonic balance method. More recently, Jao et al. [28] developed an iterative successive linearization approach based on energy optimization for estimating response statistics of beams undergoing moderately large vibrations, endowed with a fractional derivative, and subjected to combined harmonic and random excitations.

In several engineering applications, such as track dynamics, bridge design, etc, the response analysis of elastic beams subjected to moving loads is of interest. In this context, fractional calculus has been used to model the viscoelastic constitutive behaviour of beam material or to capture the rheological properties of viscoelastic foundations. By combining Laplace transform with classical modal analysis, Abu-Mallouh et al. [29] developed an analytical approach to determine transverse vibrations of Euler–Bernoulli beams with fractional derivative damping subjected to a load moving at a constant speed. In Ref. [30], the dynamic response of a simply supported Euler–Bernoulli beam with fractional derivative viscoelastic Kelvin-Voigt material model subjected to a load moving at a constant acceleration was studied by using fractional Green's function. Praharaj and Datta [31] investigated the dynamic behaviour of an Euler–Bernoulli beam resting on a fractional Kelvin–Voigt foundation subjected to a moving point load. The modal superposition method and Triangular strip matrix approach [32] were applied to solve the fractional differential equation of motion and determine dynamic response spectra. More recently, assuming a fractional Kelvin-Voigt constitutive model, the same authors [33] determined the response spectra of viscoelastic beams subjected to a moving load, as a function of the fractional derivative order. The dynamic analysis of Rayleigh beams resting on fractional viscoelastic Pasternak foundations subjected to moving loads was addressed in Ref. [34] by an analytical and numerical approach. Ouzizi et al. [35] performed nonlinear dynamic analysis of beams with geometrical nonlinearities resting on nonlinear fractional viscoelastic foundations subjected to a moving load with variable speed. The set of coupled nonlinear fractional differential equations obtained by applying Galerkin method was solved by a numerical approach based on the central difference scheme and a discrete approximation of the fractional derivative.

The numerical integration of fractional differential equations like those governing the motion of beams with fractional derivative elements crossed by moving loads might be computationally intensive. Indeed, due to the non-local character of fractional operators, the fractional derivative of the relevant variables at each time step involves the whole past time-history. Therefore, the computational effort and the storage requirements escalate with time. The use of time steps of small size may lead to prohibitive computational burden, especially for long time-histories. Numerical integration schemes adopted in the literature rely on suitable discrete approximations of the fractional derivative (see e.g., Refs. [36–41]). The accurate and efficient numerical solution of fractional differential equations is crucial to address the time-domain analysis of multi-degree-of-freedom systems with fractional derivative elements.

This paper deals with the time-domain analysis of moderately large vibrations of beams endowed with a fractional derivative element crossed by moving loads. A Galerkin-type solution procedure is applied by representing beam transversal displacement as the superposition of the linear modes of vibration and time-dependent generalized coordinates. The set of coupled nonlinear fractional differential equations governing the time-dependent generalized coordinates is solved numerically by developing a novel step-by-step scheme, labeled *improved pseudo-force method* (*IPFM*). This procedure may be viewed as the extension to nonlinear multi-degree-of-freedom systems of an integration scheme recently proposed for the time-domain analysis of fractional oscillators [42]. The latter in turn stems from the extension of an unconditionally stable numerical method for the solution of classical differential equations [43–45], which is able to achieve the same degree of accuracy as classical step-by-step integration schemes, like the *finite difference method* (*FDM*), using larger time steps.

Numerical results concerning a simply supported beam crossed by a load moving at constant speed are presented. The accuracy of the *IPFM* is assessed by comparison with the classical Newmark-β method. Parametric studies focusing on the influence of the order and coefficient of the fractional derivative on nonlinear beam vibrations are carried out.

The rest of the paper is organized as follows: in Section 2, the equation of motion of a nonlinear beam endowed with a fractional derivative element crossed by moving loads is derived and a Galerkin-type solution procedure is outlined; in Section 3, the proposed step-by-step integration scheme is developed; in Section 4, numerical results are presented; finally, in Section 5, some concluding remarks are given.

2. Problem formulation

2.1. Equation of motion

Let us consider a homogeneous simply supported Euler-Bernoulli beam of length L with cross-sectional area A, Young's modulus E, mass density ρ, and moment of inertia J. The beam is endowed with a fractional derivative element and is crossed by n_v loads, $F_i(t)$ ($i=1,2,\ldots,n_v$) moving from left to right with arbitrary velocity. Under the assumption of moderately large vibrations, the equation of motion of the beam can be written as:

$$\rho\, A\, \frac{\partial^2 v(z,t)}{\partial t^2} + E\, J\, \frac{\partial^4 v(z,t)}{\partial z^4} + c_\alpha\, {}_0^C\mathscr{D}_t^\alpha \langle v(z,t)\rangle - N\, \frac{\partial^2 v(z,t)}{\partial z^2} = \sum_{i=1}^{n_v} \chi(z_i(t))\, F_i(t)\, \delta(z - z_i(t)) \tag{1}$$

where t and z denote the time and the spatial coordinate measured along the axis of the beam (see Fig. 1), respectively; $v(z,t)$ is the transversal displacement positive if downward; N is the axial force derived under the assumption of negligible axial inertia forces and immovable end supports, i.e. (see e.g., Ref. [26]):

$$N = \frac{EA}{2L}\int_0^L \left(\frac{\partial v(z,t)}{\partial z}\right)^2 \mathrm{d}z. \tag{2}$$

In Eq. (1), ${}_0^C\mathscr{D}_t^\alpha\langle\cdot\rangle$ denotes Caputo's fractional derivative of order α,

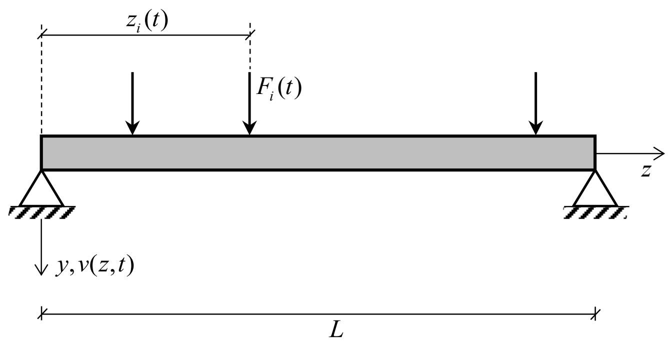

Fig. 1. Simply supported beam crossed by moving loads.

defined for a generic function $f(t)$ as [1]:

$$ {}_0^C\mathscr{D}_t^\alpha\langle f(t)\rangle = \frac{1}{\Gamma(1-\alpha)}\int_0^t (t-\tau)^{-\alpha}\frac{\mathrm{d}f(\tau)}{\mathrm{d}t}\ \mathrm{d}\tau, 0\le\alpha<1 \tag{3}$$

where $\Gamma(\cdot)$ is the Euler's gamma function. The main advantage of Caputo's fractional differential operator in engineering applications is that it leads to physically meaningful initial conditions which take on the same form as for integer-order differential equations [1]. It is worth mentioning that, if the structural system is quiescent at time $t = 0$, or the system operates from $t = -\infty$, the Riemann–Liouville and Caputo's fractional operators give the same result.

The fractional derivative term in Eq. (1), with coefficient c_α and derivative order $0 \le \alpha < 1$, can describe an externally distributed stiffness/damping [26,27], including a viscoelastic foundation (see e.g., Refs. [14,24]). In the limiting cases when $\alpha = 0$ and $\alpha = 1$, the fractional derivative term represents a restoring force and classical viscous damping, respectively.

On the right-hand side of Eq. (1), $z_i(t)$ denotes the instantaneous position of the $i-$th moving force; and $\chi(z)$ is the so-called *window function*, given by:

$$\chi(z) = \mathscr{U}(z) - \mathscr{U}(z-L) \tag{4}$$

$\mathscr{U}(z)$ being the unit-step function, defined in such a way that $\mathscr{U}(z) = 0$ when $z < 0$; $\mathscr{U}(z) = 1/2$ at $z = 0$; $\mathscr{U}(z) = 1$ when $z > 0$; and $\delta(z) = \partial\mathscr{U}(z)/\partial z$ is the Dirac's delta function, symmetric with respect to $z = 0$. For the simply supported beam, the boundary conditions read $v(z,t)|_{z=0} = v(z,t)|_{z=L} = 0$ and $\partial^2 v(z,t)/\partial z^2|_{z=0} = \partial^2 v(z,t)/\partial z^2|_{z=L} = 0$. It is assumed that the beam is at rest for $t \le 0$ and that the first load enters the beam from the left-hand support at $t = 0$. Therefore, Eq. (1) is supplemented by homogeneous initial conditions.

Step-by-step algorithms for the numerical integration of fractional differential equations rely on discretized forms of the fractional derivative (see e.g., Refs. [36–41]). If the time interval of interest $[0, T]$ is subdivided into M small intervals of equal length $\Delta t = T/M$, such that $t_0 = 0, t_1 = \Delta t, \dots, t_n = n\Delta t, \dots, t_M = M\Delta t$ are the subdivision times, Caputo's fractional derivative of the function $f(t)$ at the time instant t_n can be expressed in the following discretized form, known as *Grünwald–Letnikov* (*GL*) approximation or G1-algorithm [1,46]:

$$ {}_0^{GL}\mathscr{D}_t^\alpha\langle f(t_n)\rangle \cong \frac{1}{(\Delta t)^\alpha}\sum_{j=1}^{n}\lambda_j(\alpha)\ f\left(t_{n+1-j}\right) \tag{5}$$

where the coefficients $\lambda_j(\alpha)$ may be evaluated in recursive form:

$$\lambda_1(\alpha) = 1, \lambda_2(\alpha) = -\alpha, \dots, \lambda_j(\alpha) = \left(\frac{j-2-\alpha}{j-1}\right)\lambda_{j-1}(\alpha), \dots, \quad j = 3, 4, \dots, n. \tag{6}$$

Equation (5) reflects the *long tail memory* or non-local character of fractional differential operators by expressing the fractional derivative of the function $f(t)$ at the generic time instant t_n as a summation of all past values of the function weighted by the *GL* coefficients $\lambda_j(\alpha)$.

2.2. Galerkin method

An approximate solution of Eq. (1) can be obtained by applying a Galerkin-type procedure. In this context, the transversal displacement field of the beam is expressed as:

$$v(z,t) = \sum_{k=1}^{n_b}\varphi_k(z)q_k(t) = \boldsymbol{\varphi}^{\mathrm{T}}(z)\mathbf{q}(t) \tag{7}$$

where $\boldsymbol{\varphi}(z)$ and $\mathbf{q}(t)$ are the vectors collecting n_b basis functions, $\varphi_k(z)$, and the associated time-dependent generalized coordinates, $q_k(t)$, respectively.

An appropriate choice for the basis functions is represented by the eigenfunctions of the associated linear problem which are the solutions of the following eigenvalue problem:

$$E\ J\ \varphi_j^{IV}(z) = \rho A\omega_j^2\varphi_j(z) \tag{8}$$

where ω_j denotes the $j-$th natural circular frequency. Equation (8) has to be solved in conjunction with the pertinent boundary conditions. As known, for the simply supported beam, the $j-$th linear modal shape, orthonormal with respect to the mass per unit length ρA, reads $\varphi_j(z) = \sqrt{2/(\rho AL)}\sin(j\,\pi\,z/L)$, and the associated natural frequency is $\omega_j = (j\,\pi/L)^2\sqrt{EJ/(\rho A)}$.

Substituting Eq. (7) into Eq. (1), pre-multiplying the resulting equation by $\varphi_j(z)$ and integrating with respect to z from 0 to L, the following set of n_b coupled nonlinear fractional differential equations governing the time variation of the generalized coordinates is obtained:

$$\ddot{q}_j(t) + \omega_j^2\ q_j(t) + \frac{c_\alpha}{\rho A}\,{}_0^C\mathscr{D}_t^\alpha\langle q_j(t)\rangle - \frac{EA}{2L}\sum_{k=1}^{n_b}\sum_{s=1}^{n_b}\sum_{m=1}^{n_b}R_{jk}S_{sm}q_k(t)q_s(t)q_m(t) = \sum_{i=1}^{n_v}\chi(z_i(t))\ F_i(t)\ \varphi_j(z_i(t)), j = 1, 2, \dots, n_b \tag{9}$$

where the over-dot denotes the total derivative with respect to time t; R_{jk} and S_{sm} are defined as

$$R_{jk} = \int_0^L \varphi_j(z)\varphi''_k(z)\mathrm{d}z \tag{10a}$$

$$S_{sm} = \int_0^L \varphi'_s(z)\varphi'_m(z)\mathrm{d}z \tag{10b}$$

where the apex denotes the total derivative with respect to the spatial variable z and the orthogonality condition of the linear modes of vibration has been exploited i.e.:

$$\int_0^L \varphi_j(z)\varphi_k(z)\mathrm{d}z = \frac{\delta_{jk}}{\rho A} \tag{11}$$

δ_{jk} being the Kronecker delta.

Equation (9) can be recast in matrix form as follows

$$\ddot{\mathbf{q}}(t) + \boldsymbol{\Omega}^2\ \mathbf{q}(t) + \frac{c_\alpha}{\rho A}\,{}_0^C\mathscr{D}_t^\alpha\langle\mathbf{q}(t)\rangle + \mathbf{p}_{\mathrm{NL}}(\mathbf{q}(t)) = \mathbf{f}_{\mathrm{v}}(t) \tag{12}$$

where $\boldsymbol{\Omega}^2$ is a diagonal matrix listing the squares of the first n_b natural frequencies of the linear beam; $\mathbf{p}_{\mathrm{NL}}(\mathbf{q}(t))$ is the vector collecting the nonlinear restoring forces defined as:

$$\mathbf{p}_{\rm NL}(\mathbf{q}(t)) = -\frac{EA}{2L}\mathbf{q}^{\rm T}(t)\mathbf{S}\mathbf{q}(t)\mathbf{R}\mathbf{q}(t) \tag{13}$$

where $\mathbf{R}$ and $\mathbf{S}$ are $(n_b \times n_b)$ matrices whose elements are defined in Eqs. (10 a,b) . Finally, the vector $\mathbf{f}_{\rm v}(t)$ in Eq. (12) is given by:

$$\mathbf{f}_{\rm v}(t) = \mathbf{\Phi}(t)\mathbf{X}(t)\mathbf{F}(t) \tag{14}$$

where

$$\begin{aligned}
\mathbf{\Phi}(t) &= [\boldsymbol{\varphi}(z_1(t)) \quad \boldsymbol{\varphi}(z_2(t)) \quad \dots \quad \boldsymbol{\varphi}(z_{n_v}(t))];\\
\mathbf{X}(t) &= \mathrm{Diag}[\chi(z_1(t)) \quad \chi(z_2(t)) \quad \dots \quad \chi(z_{n_v}(t))];\\
\mathbf{F}(t) &= [F_1(t) \quad F_2(t) \quad \dots \quad F_{n_v}(t)]^{\rm T}.
\end{aligned} \tag{15}$$

2.3. State variables formulation

Equation (12) can be rewritten in terms of state variables as follows:

$$\dot{\mathbf{z}}(t) = \mathbf{D}_{\rm L}\mathbf{z}(t) + \mathbf{V}_\alpha\, {}_0^C\mathscr{D}_t^\alpha\langle\mathbf{z}(t)\rangle + \mathbf{P}_{\rm NL}(\mathbf{q}(t)) + \mathbf{F}_{\rm v}(t) \tag{16}$$

where

$$\begin{aligned}
&\mathbf{z}(t) = \begin{Bmatrix}\mathbf{q}(t)\\ \dot{\mathbf{q}}(t)\end{Bmatrix};\quad \mathbf{D}_{\rm L} = \begin{bmatrix}\mathbf{0} & \mathbf{I}_{n_b}\\ -\mathbf{\Omega}^2 & \mathbf{0}\end{bmatrix};\quad \mathbf{V}_\alpha = \begin{bmatrix}\mathbf{0} & \mathbf{0}\\ -\dfrac{c_\alpha}{\rho A}\mathbf{I}_{n_b} & \mathbf{0}\end{bmatrix};\\
&\mathbf{P}_{\rm NL}(\mathbf{q}(t)) = \begin{Bmatrix}\mathbf{0}\\ -\mathbf{p}_{\rm NL}(\mathbf{q}(t))\end{Bmatrix};\quad \mathbf{F}_{\rm v}(t) = \begin{Bmatrix}\mathbf{0}\\ \mathbf{f}_{\rm v}(t)\end{Bmatrix}
\end{aligned} \tag{17}$$

with $\mathbf{I}_{n_b}$ denoting the identity matrix of order n_b.

Let the motion start at $t_0 = 0$ and be $\mathbf{z}_0 = \mathbf{z}(0)$ the vector collecting the initial conditions. The solution of Eq. (16) can be formally written as:

$$\mathbf{z}(t) = \mathbf{\Theta}_{\rm L}(t-t_0)\mathbf{z}_0 + \int_{t_0}^{t} \mathbf{\Theta}_{\rm L}(t-\tau)\ \mathbf{F}_\alpha(\tau;\mathbf{q}(\tau))\ d\tau \tag{18}$$

where

$$\mathbf{\Theta}_{\rm L}(t) = \exp(\mathbf{D}_{\rm L}\, t) = \begin{bmatrix}-\mathbf{g}(t)\mathbf{\Omega}^2 & \mathbf{h}(t)\\ -\mathbf{h}(t)\mathbf{\Omega}^2 & \dot{\mathbf{h}}(t)\end{bmatrix} \tag{19}$$

is the *transition matrix* of the undamped linear system with $\mathbf{g}(t)$, $\mathbf{h}(t)$, and $\dot{\mathbf{h}}(t)$ denoting diagonal matrices whose $j-$th elements read:

$$\begin{aligned}
g_j(t) &= -\frac{1}{\omega_j^2}\cos(\omega_j t);\\
h_j(t) &= \dot{g}_j(t) = \frac{1}{\omega_j}\sin(\omega_j t);\\
\dot{h}_j(t) &= \cos(\omega_j t).
\end{aligned} \tag{20}$$

The vector $\mathbf{F}_\alpha(\tau;\mathbf{q}(\tau))$ in Eq. (18), defined as

$$\mathbf{F}_\alpha(t;\mathbf{q}(t)) = \mathbf{V}_\alpha\, {}_0^C\mathscr{D}_t^\alpha\langle\mathbf{z}(t)\rangle + \mathbf{P}_{\rm NL}(\mathbf{q}(t)) + \mathbf{F}_{\rm v}(t) \tag{21}$$

may be viewed as a *pseudo-force* vector. Indeed, in Eq. (21) $\mathbf{F}_{\rm v}(t)$ is the known force vector due to the moving loads, while the first two terms on the right-hand side are a priori unknown since they depend on the unknown system response.

3. Time-domain numerical integration

3.1. Improved pseudo-force method

In this section, a novel step-by-step integration procedure for the numerical solution of the set of coupled nonlinear fractional differential equations in Eq. (16) is proposed. The procedure is derived by extending the step-by-step integration scheme recently developed by Sofi and Muscolino [42] for the time-domain response analysis of nonlinear fractional oscillators subjected to arbitrary dynamic excitation. In turn, this approach stems from the extension of a method originally proposed in Refs. [43,44] for classical linear differential equations to the solution of equations involving nonlinearities and fractional derivatives.

Let the time interval of interest $[0, T]$ be subdivided into small intervals of equal length $\Delta t = T/M$, with $t_0 = 0, t_1 = \Delta t, \dots, t_n = n\Delta t, t_{n+1} = (n+1)\Delta t, \dots, t_M = M\Delta t$ denoting the subdivision times.

By assuming t_n as initial time instant of the motion in the interval $[t_n, t_{n+1}]$, Eq. (18) yields the state variable vector at the time instant t_{n+1} in the following form:

$$\mathbf{z}(t_{n+1}) = \mathbf{\Theta}_{\rm L}(\Delta t)\mathbf{z}(t_n) + \int_{t_n}^{t_{n+1}} \mathbf{\Theta}_{\rm L}(t_{n+1}-\tau)\ \mathbf{F}_\alpha(\tau;\mathbf{q}(\tau))\ d\tau \tag{22}$$

where the first term on the right-hand side depends on the solution at t_n; the second term involves a convolution integral which represents the aliquot of the solution due to the *pseudo-force* vector (see Eq. (21)). The evaluation of this convolution integral requires a suitable interpolation of the *pseudo-force* vector within the time interval $[t_n, t_{n+1}]$.

By assuming that the *pseudo-force* vector, $\mathbf{F}_\alpha(t;\mathbf{q}(t))$, is piecewise linear in each time interval, Eq. (22) yields the following expression of the state variable vector at the time instant t_{n+1} [45]:

$$\begin{aligned}
\mathbf{z}(t_{n+1}) = {} & \mathbf{\Theta}_{\rm L}(\Delta t)\mathbf{z}(t_n) + \boldsymbol{\gamma}_0(\Delta t)\mathbf{F}_\alpha(t_n;\mathbf{q}(t_n))\\
& + \boldsymbol{\gamma}_1(\Delta t)\mathbf{F}_\alpha(t_{n+1};\mathbf{q}(t_{n+1}))
\end{aligned} \tag{23}$$

where

$$\mathbf{L}_{\rm L}(\Delta t) = \left[\mathbf{\Theta}_{\rm L}(\Delta t) - \mathbf{I}_{2n_b}\right](\mathbf{D}_{\rm L})^{-1} \tag{24a}$$

$$\boldsymbol{\gamma}_0(\Delta t) = \left[\mathbf{\Theta}_{\rm L}(\Delta t) - \frac{1}{\Delta t}\mathbf{L}_{\rm L}(\Delta t)\right](\mathbf{D}_{\rm L})^{-1} \tag{24b}$$

$$\boldsymbol{\gamma}_1(\Delta t) = \left[\frac{1}{\Delta t}\mathbf{L}_{\rm L}(\Delta t) - \mathbf{I}_{2n_b}\right](\mathbf{D}_{\rm L})^{-1} \tag{24c}$$

where $\mathbf{I}_{2n_b}$ is the identity matrix of order $2n_b$.

Since the set of coupled nonlinear fractional differential equations (16) has homogeneous initial conditions, Caputo's fractional operator can be replaced by the GL operator [38]. As a result, the *pseudo-force* vector (see Eq. (21)), at the two successive time instants t_n and t_{n+1}, reads:

$$\mathbf{F}_\alpha(t_i;\mathbf{q}(t_i)) = \mathbf{V}_\alpha\, {}_0^{GL}\mathscr{D}_t^\alpha\langle\mathbf{z}(t_i)\rangle + \mathbf{P}_{\rm NL}(\mathbf{q}(t_i)) + \mathbf{F}_{\rm v}(t_i),\ i = n, n+1. \tag{25}$$

By using the *GL* approximation in Eq. (5), with the same discretization of the time interval of interest as the one adopted for numerical integration purposes, the term depending on the fractional derivative in Eq. (25), evaluated at the time instants t_n and t_{n+1}, is expressed as follows:

$${}_0^{GL}\mathscr{D}_t^\alpha\langle\mathbf{z}(t_n)\rangle = \frac{1}{(\Delta t)^\alpha}\sum_{j=1}^{n}\lambda_j(\alpha)\mathbf{z}(t_{n+1-j}) \tag{26a}$$

$$\begin{aligned}
{}_0^{GL}\mathscr{D}_t^\alpha\langle\mathbf{z}(t_{n+1})\rangle &= \frac{1}{(\Delta t)^\alpha}\sum_{j=1}^{n+1}\lambda_j(\alpha)\ \mathbf{z}(t_{n+2-j})\\
&= \frac{1}{(\Delta t)^\alpha}\ \mathbf{z}(t_{n+1}) + \frac{1}{(\Delta t)^\alpha}\sum_{j=2}^{n+1}\lambda_j(\alpha)\mathbf{z}(t_{n+2-j}).
\end{aligned} \tag{26b}$$

By substituting Eqs. (25) and (26 a,b) into Eq. (23), the following expression of the state variable vector at the time instant t_{n+1} is obtained:

$$\begin{aligned}\mathbf{z}(t_{n+1}) &= \mathbf{\Theta}_{\mathrm{L}}(\Delta t)\mathbf{z}(t_n)\\ &+\boldsymbol{\gamma}_0(\Delta t)\left[\frac{\mathbf{V}_\alpha}{(\Delta t)^\alpha}\sum_{j=1}^{n}\lambda_j(\alpha)\;\mathbf{z}\left(t_{n+1-j}\right)+\mathbf{P}_{\mathrm{NL}}(\mathbf{q}(t_n))+\mathbf{F}_{\mathrm{v}}(t_n)\right]\\ &+\boldsymbol{\gamma}_1(\Delta t)\left[\frac{\mathbf{V}_\alpha}{(\Delta t)^\alpha}\mathbf{z}(t_{n+1})+\frac{\mathbf{V}_\alpha}{(\Delta t)^\alpha}\sum_{j=2}^{n+1}\lambda_j(\alpha)\;\mathbf{z}\left(t_{n+2-j}\right)\right.\\ &\left.+\mathbf{P}_{\mathrm{NL}}(\mathbf{q}(t_{n+1}))+\mathbf{F}_{\mathrm{v}}(t_{n+1})\right].\end{aligned} \tag{27}$$

By solving the previous equation with respect to the state variable vector $\mathbf{z}(t_{n+1})$, the following step-by-step integration scheme is obtained:

Table 1
Geometrical and mechanical properties of the beam crossed by the moving load.

Parameter	Value
E	$2.1\times10^{11}\,\mathrm{N/m^2}$
ρ	$2355\ \mathrm{kg/m^3}$
c_α	$10^4\ \mathrm{Ns^\alpha/m^2}$
L	$20\ \mathrm{m}$
A	$0.03\mathrm{m^2}$
J	$2.25\times10^{-4}\ \mathrm{m^4}$

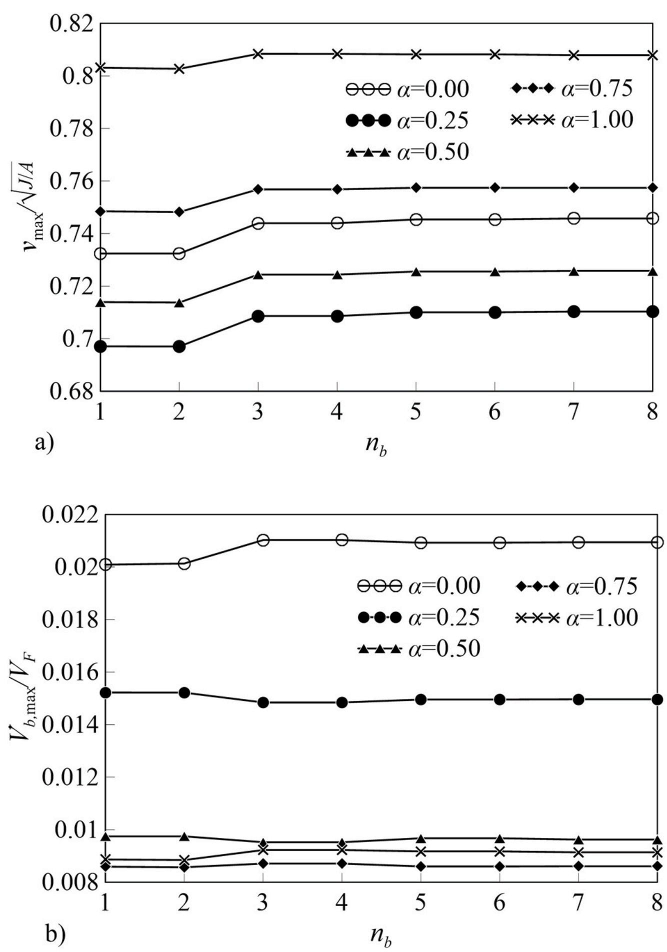

Fig. 2. Maximum normalized midspan (a) displacement and (b) velocity of the beam versus the number of linear vibration modes n_b for different values of the fractional derivative order α ($V_F = 10$ m/s, $\Delta t = 0.001$ s).

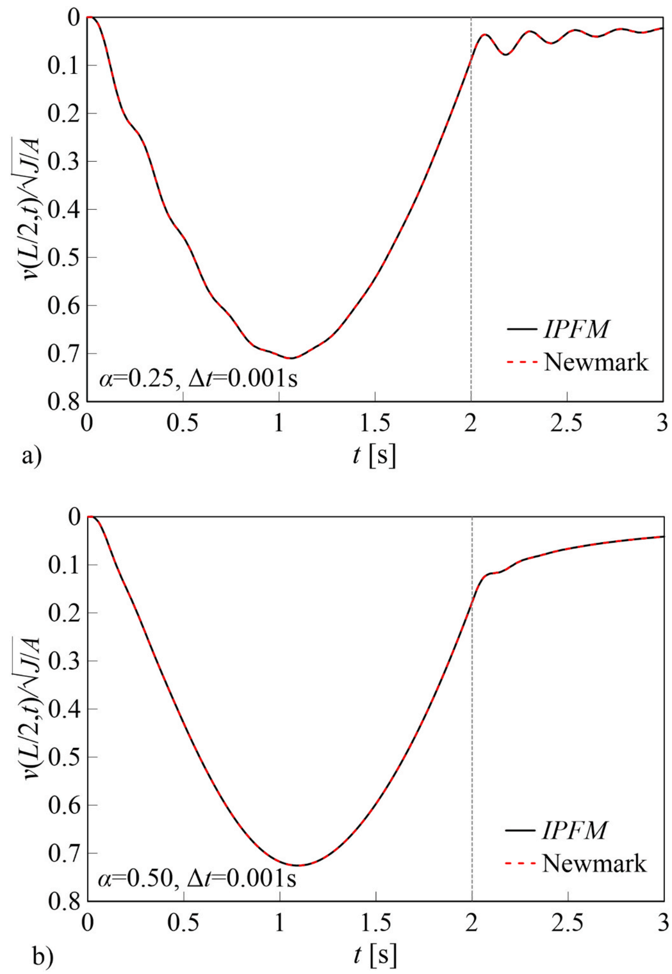

Fig. 3. Time-history of beam normalized midspan displacement obtained by the *IPFM* and Newmark-β method: a) $\alpha = 0.25$; b) $\alpha = 0.50$ ($V_F = 10$ m/s).

$$\begin{aligned}\mathbf{z}(t_{n+1}) &= \widetilde{\mathbf{\Theta}}_{\mathrm{L}}(\Delta t)\mathbf{z}(t_n)\\ &+\widetilde{\boldsymbol{\gamma}}_0(\Delta t)\left[\frac{\mathbf{V}_\alpha}{(\Delta t)^\alpha}\sum_{j=1}^{n}\lambda_j(\alpha)\;\mathbf{z}\left(t_{n+1-j}\right)+\mathbf{P}_{\mathrm{NL}}(\mathbf{q}(t_n))+\mathbf{F}_{\mathrm{v}}(t_n)\right]\\ &+\widetilde{\boldsymbol{\gamma}}_1(\Delta t)\left[\frac{\mathbf{V}_\alpha}{(\Delta t)^\alpha}\sum_{j=2}^{n+1}\lambda_j(\alpha)\;\mathbf{z}\left(t_{n+2-j}\right)+\mathbf{P}_{\mathrm{NL}}(\mathbf{q}(t_{n+1}))+\mathbf{F}_{\mathrm{v}}(t_{n+1})\right]\end{aligned} \tag{28}$$

where

$$\mathbf{\Psi}(\Delta t)=\left[\mathbf{I}_{2n_b}-\frac{1}{(\Delta t)^\alpha}\boldsymbol{\gamma}_1(\Delta t)\mathbf{V}_\alpha\right]^{-1} \tag{29a}$$

$$\widetilde{\mathbf{\Theta}}_{\mathrm{L}}(\Delta t)=\mathbf{\Psi}(\Delta t)\mathbf{\Theta}_{\mathrm{L}}(\Delta t) \tag{29b}$$

$$\widetilde{\boldsymbol{\gamma}}_0(\Delta t)=\mathbf{\Psi}(\Delta t)\boldsymbol{\gamma}_0(\Delta t) \tag{29c}$$

$$\widetilde{\boldsymbol{\gamma}}_1(\Delta t)=\mathbf{\Psi}(\Delta t)\boldsymbol{\gamma}_1(\Delta t). \tag{29d}$$

It can be observed that the state variable vector $\mathbf{z}(t_{n+1})$ at the time instant t_{n+1} depends on the unknown generalized coordinates $\mathbf{q}(t_{n+1})$ through the vector $\mathbf{P}_{\mathrm{NL}}(\mathbf{q}(t_{n+1}))$ resulting from the nonlinear bending behavior of the beam. It follows that an iterative procedure is needed to evaluate $\mathbf{z}(t_{n+1})$ by means of Eq. (28). At the first iteration, it is assumed:

$$\mathbf{P}_{\mathrm{NL}}^{(1)}(\mathbf{q}(t_{n+1}))=\mathbf{P}_{\mathrm{NL}}(\mathbf{q}(t_n)). \tag{30}$$

At the second iteration:

$$\mathbf{P}_{\mathrm{NL}}^{(2)}(\mathbf{q}(t_{n+1}))=\mathbf{P}_{\mathrm{NL}}\left(\mathbf{q}^{(1)}(t_{n+1})\right) \tag{31}$$

and so on. The $(i+1)-$th iteration, with $i\geq 1$, is carried out by setting:

$$\mathbf{P}_{\mathrm{NL}}^{(i+1)}(\mathbf{q}(t_{n+1}))=\mathbf{P}_{\mathrm{NL}}\left(\mathbf{q}^{(i)}(t_{n+1})\right) \tag{32}$$

where the superscript in parenthesis denotes the iteration number.

Iterations can be stopped when the following condition is satisfied:

$$\left|\frac{\left\|\mathbf{z}^{(i+1)}(t_{n+1})\right\|_2-\left\|\mathbf{z}^{(i)}(t_{n+1})\right\|_2}{\left\|\mathbf{z}^{(i+1)}(t_{n+1})\right\|_2}\right|\leq\delta_c \tag{33}$$

where $|\cdot|$ and $\|\cdot\|_2$ denote the absolute value and the Euclidean norm, respectively; δ_c is a preset tolerance.

It is worth emphasizing that, under the assumption of small amplitude vibrations, nonlinear terms in the equation of motion of the beam are negligible and Eq. (28) takes the following form:

$$\begin{aligned}\mathbf{z}(t_{n+1})=&\widetilde{\boldsymbol{\Theta}}_{\mathrm{L}}(\Delta t)\mathbf{z}(t_n)+\widetilde{\boldsymbol{\gamma}}_0(\Delta t)\left[\frac{\mathbf{V}_\alpha}{(\Delta t)^\alpha}\sum_{j=1}^{n}\lambda_j(\alpha)\ \mathbf{z}(t_{n+1-j})+\mathbf{F}_{\mathrm{v}}(t_n)\right]\\&+\widetilde{\boldsymbol{\gamma}}_1(\Delta t)\left[\frac{\mathbf{V}_\alpha}{(\Delta t)^\alpha}\sum_{j=2}^{n+1}\lambda_j(\alpha)\ \mathbf{z}(t_{n+2-j})+\mathbf{F}_{\mathrm{v}}(t_{n+1})\right].\end{aligned} \tag{34}$$

Equation (34) provides an explicit step-by-step integration scheme which does not require any iteration.

Once the state variable vector $\mathbf{z}(t_{n+1})$ in the generalized coordinate space at the time instant t_{n+1} is known, the state variable vector of beam response $\mathbf{y}(z,t_{n+1})=\left[v(z,t_{n+1})\quad \dot{v}(z,t_{n+1})\right]^{\mathrm{T}}$ at the same time instant can be determined as follows:

$$\mathbf{y}(z,t_{n+1})=\begin{bmatrix}\boldsymbol{\varphi}^{\mathrm{T}}(z) & \mathbf{0}\\ \mathbf{0} & \boldsymbol{\varphi}^{\mathrm{T}}(z)\end{bmatrix}\mathbf{z}(t_{n+1}) \tag{35}$$

for any value of the spatial coordinate z.

Summarizing, the proposed procedure for the time-domain analysis of moderately large vibrations of beams endowed with fractional derivative elements involves the following main steps: *i*) to represent beam transversal displacement as the superposition of the linear modes of vibration and time-dependent generalized coordinates; *ii*) to approximate the fractional derivative of the solution at each time instant by means of the *GL* representation which involves the whole past history; *iii*) to treat terms depending on the unknown solution at the current time instant, which result from the *GL* representation as well as from nonlinearities, as *pseudo-forces*; *iv*) to perform iterations at each time step to handle nonlinear terms resulting from moderately large vibrations of the beam; *v*) to determine beam transversal displacement at each time step once the time-dependent generalized coordinates are known.

From the computational point of view, a notable feature of the *IPFM* is that the matrices in Eqs. (29 a-d) need to be computed only once since they depend on the time step size Δt and do not change over the integration process. Furthermore, unlike the classical Newmark-β method (see Appendix A), the *IPFM* does not require the evaluation of the tangent stiffness matrix at each time step.

It is worth remarking that the proposed procedure, based on the linear mode superposition approach and the *IPFM*, can be applied to determine the time-domain response of nonlinear beams endowed with fractional derivative elements subjected to arbitrary dynamic

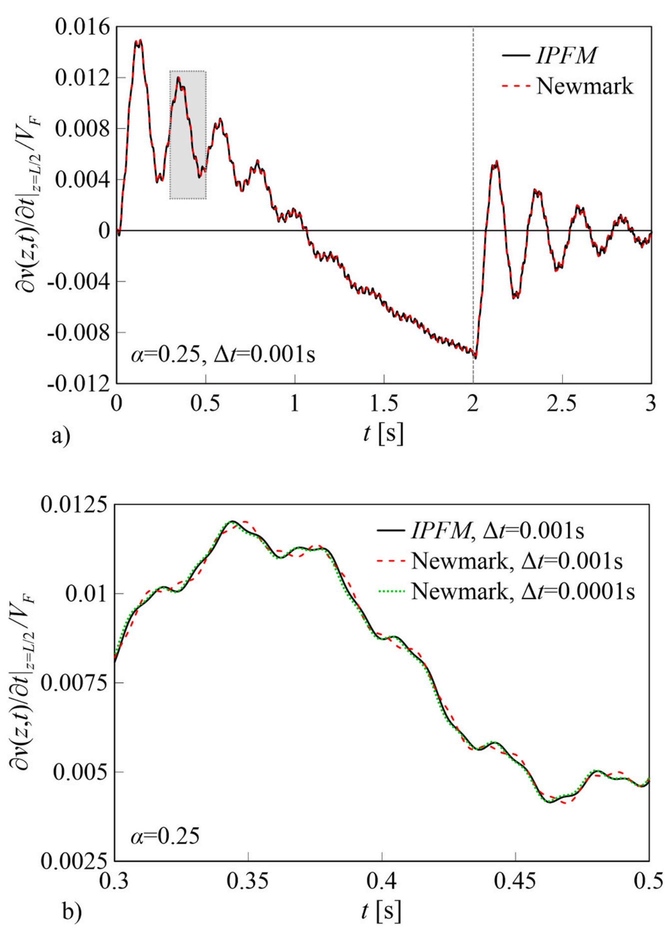

Fig. 4. Time-history of beam normalized midspan velocity: a) comparison between the *IPFM* and Newmark-β method; b) enlargement ($\alpha=0.25$; $V_F=10$ m/s).

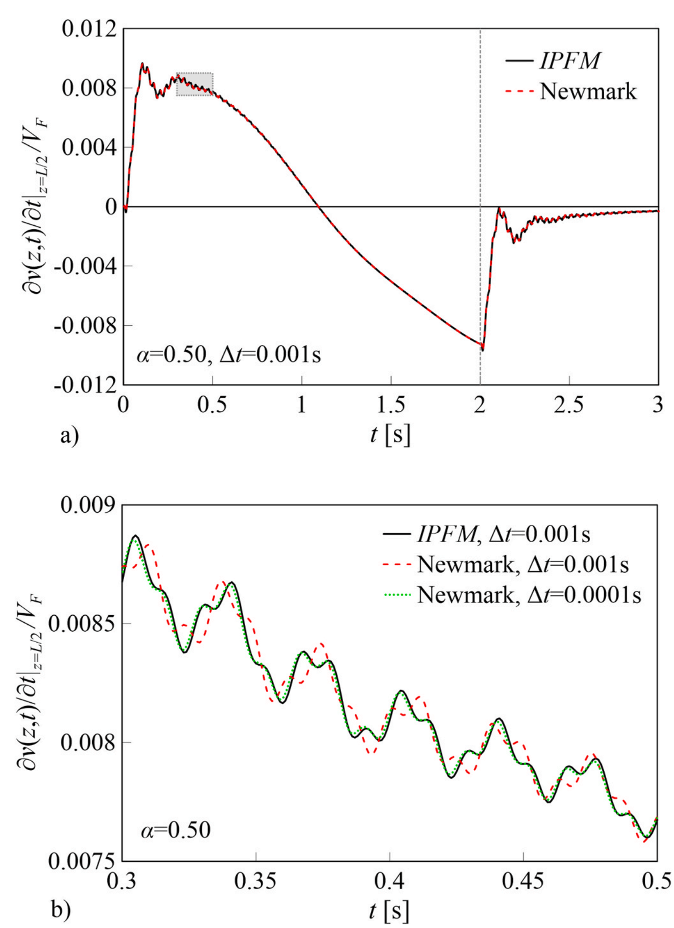

Fig. 5. Time-history of beam normalized midspan velocity: a) comparison between the *IPFM* and Newmark-β method; b) enlargement ($\alpha=0.50$; $V_F=10$ m/s).

excitations.

3.2. *Truncation of the Grünwald–Letnikov approximation*

Due to the non-local nature of the fractional differential operator, the time-domain integration of fractional differential equations by step-by-step algorithms is time-consuming. The evaluation of the response at the generic time step t_{n+1} by the proposed integration scheme in Eq. (28) requires the onerous summation of all past values of the response. As time increases, a larger number of terms is involved, and the computational cost of the whole time-integration process may become prohibitive for long time-histories.

The computational efficiency of step-by-step integration procedures for the numerical solution of fractional differential equations, including the proposed *IPFM*, can be enhanced by applying the "short memory" principle [1] which stems from the observation that the absolute value of the *GL* weights $\lambda_j(\alpha)$ (see Eq. (6)) tends to zero as the number j of the time step increases. This feature is consistent with the *fading memory* property of the fractional derivatives and allows one to truncate the *GL* approximation of the fractional derivative of the solution at the generic time instant by retaining only the contribution of the most recent time-history which largely affects the response at each time step (see e.g., Refs. [39,41,42]), i.e.

$$ {}_0^{GL}\mathscr{D}_t^{\alpha}\langle \mathbf{z}(t_n)\rangle = \begin{cases} \dfrac{1}{(\Delta t)^{\alpha}} \displaystyle\sum_{j=1}^{n} \lambda_j(\alpha)\mathbf{z}\big(t_{n+1-j}\big), \text{if } n \le n_T \\ \dfrac{1}{(\Delta t)^{\alpha}} \displaystyle\sum_{j=1}^{n_T} \lambda_j(\alpha)\mathbf{z}\big(t_{n+1-j}\big), \text{if } n > n_T \end{cases} \tag{36} $$

where n_T is the number of time instants that must be retained to achieve good accuracy.

4. Numerical application

The selected case-study concerns a simply supported beam crossed by a load of intensity $F = 25$ kN moving with constant speed $V_F = 10$ m/s, unless otherwise specified. The geometrical and mechanical properties of the beam are listed in Table 1 [26]. The normalized midspan displacement, $v(L/2,t)/\sqrt{J/A}$, and velocity, $\partial v(z,t)/\partial t|_{z=L/2}/V_F$, of the beam are selected as response quantities of interest. Different values of the fractional derivative order, α, are considered. The tolerance to assess convergence of iterations of the *IPFM* is set equal to $\delta_c = 10^{-4}$ (see Eq. (33)).

As a first step, the number of linear vibration modes n_b needed to obtain accurate predictions of the response has to be defined. Fig. 2 shows the maximum normalized midspan displacement and velocity of the beam, $v_{\max}/\sqrt{J/A}$ and $V_{b,\max}/V_F$, over the time interval $[0,3]$s versus the number of vibration modes obtained by applying the *IPFM* with a time step $\Delta t = 0.001$ s. Five different values of the fractional derivative order are considered. It can be observed that the solution does not

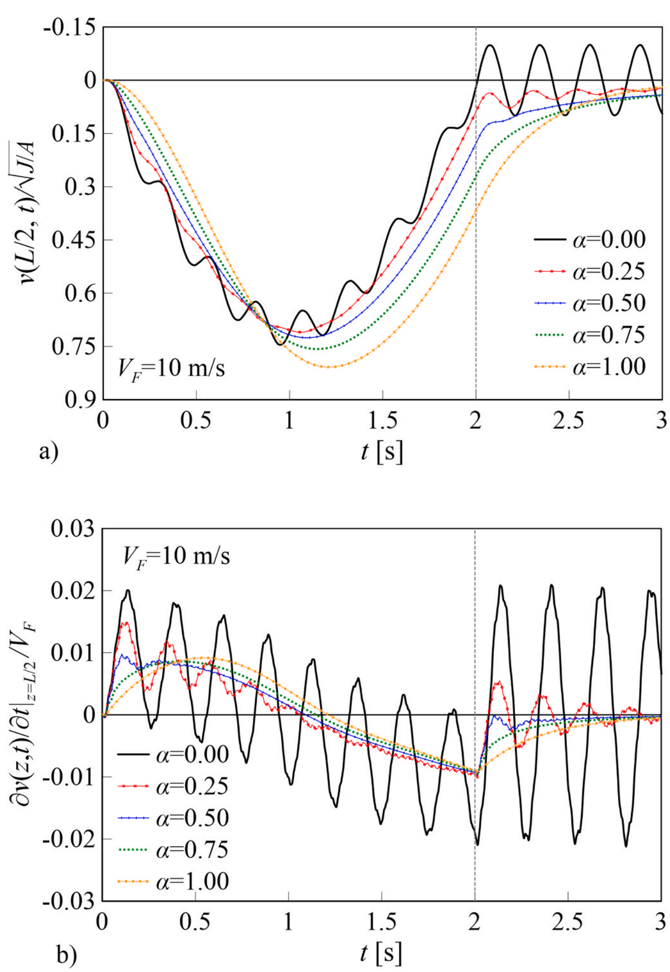

Fig. 6. Time-history of beam normalized midspan (a) displacement and (b) velocity for different values of the fractional derivative order α ($V_F = 10$ m/s).

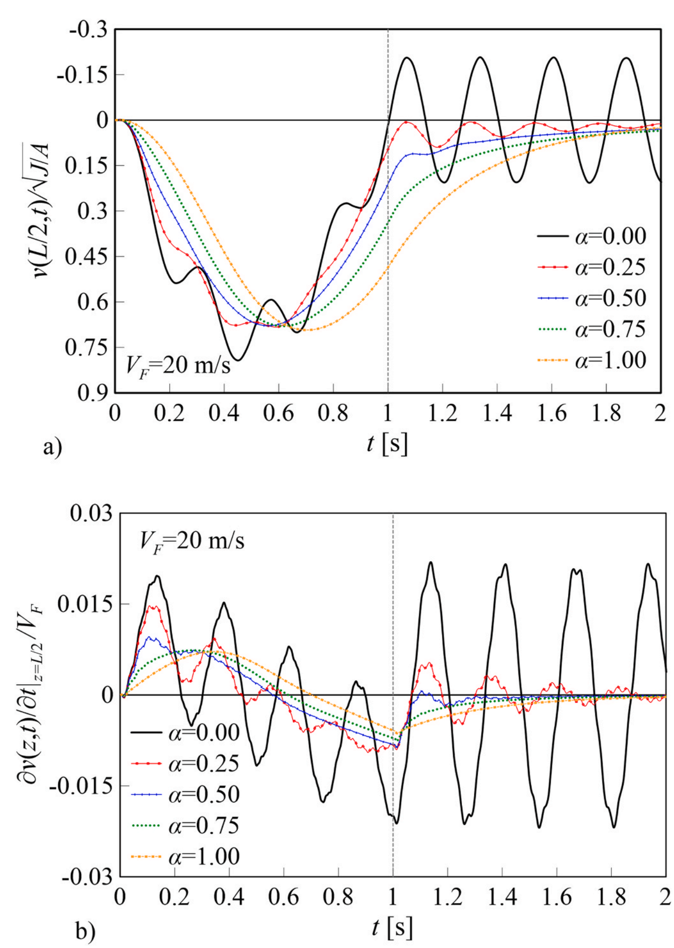

Fig. 7. Time-history of beam normalized midspan (a) displacement and (b) velocity for different values of the fractional derivative order α ($V_F = 20$ m/s).

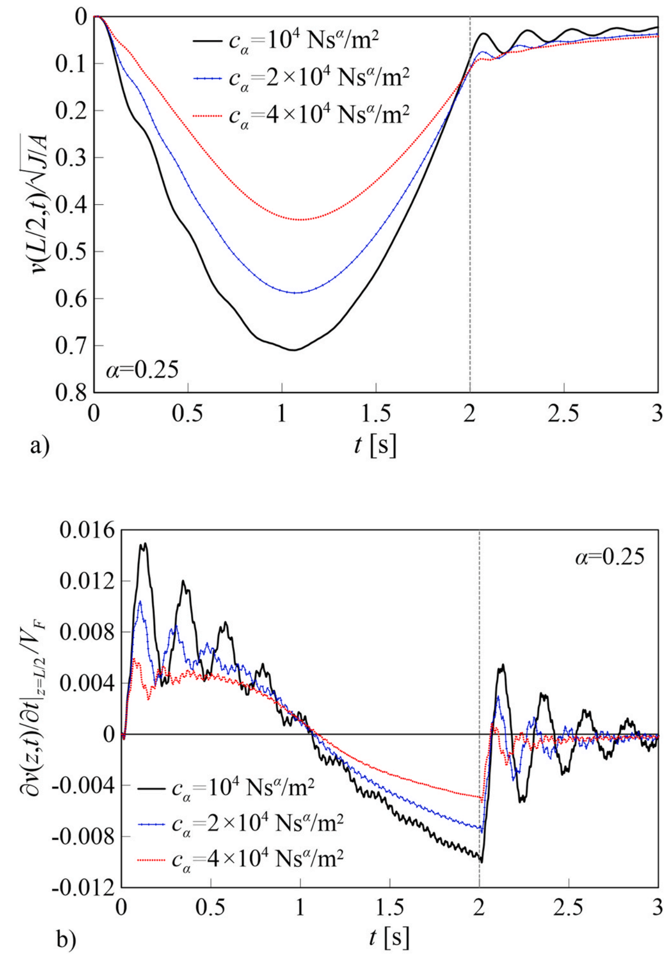

Fig. 8. Time-history of beam normalized midspan (a) displacement and (b) velocity for different values of the fractional derivative coefficient c_α ($\alpha = 0.25$, $V_F = 10$ m/s).

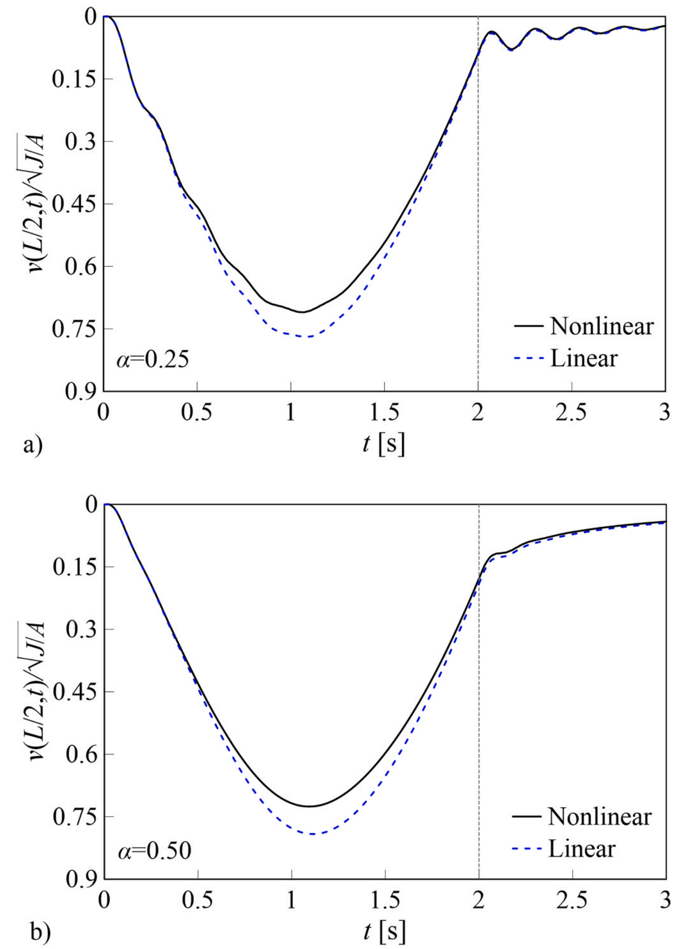

Fig. 9. Time-history of beam normalized midspan displacement obtained neglecting and retaining nonlinearities: a) $\alpha = 0.25$; b) $\alpha = 0.50$ ($V_F = 10$ m/s).

significantly change when more than five mode shapes are retained, whatever the order of the fractional derivative is. Thus, the transversal displacement of the beam is expressed by means of Eq. (7) considering the first $n_b = 5$ linear vibration modes.

The accuracy of the proposed *IPFM* is assessed by performing appropriate comparisons with the classical Newmark-β method based on the constant average acceleration assumption (see Appendix A), for two different orders of the fractional derivative, $\alpha = 0.25$ and $\alpha = 0.50$. As shown in Fig. 3, the time-histories of beam normalized midspan displacement provided by the *IPFM* and Newmark-β method assuming a time step $\Delta t = 0.001$ s are in excellent agreement. The dashed vertical line marks the time instant $t_f = L/V_F$ in which the moving force exits the beam crossing the right-hand support. It is worth mentioning that only a few iterations are required to fulfil the convergence condition in Eq. (33).

Figs. 4 and 5 display a similar comparison in terms of beam normalized midspan velocity. A good match is found over the whole time-history. By inspection of the enlargements in Figs. 4b and 5b, however, it can be observed that Newmark-β method requires a time step ten times smaller to achieve the same level of accuracy as the *IPFM*. Analogous results, omitted for conciseness, are obtained for different fractional derivative orders. Based on the comparison with Newmark-β method, it is concluded that the *IPFM* with a time step $\Delta t = 0.001$ s provides accurate estimates of both displacement and velocity.

Once the accuracy has been assessed, the *IPFM* is applied to investigate the influence of the fractional derivative order, α, and coefficient, c_α, on beam response. In Fig. 6, the time-histories of the normalized midspan displacement and velocity of the beam for five different values of the fractional derivative order are plotted. Fig. 6a shows that both the maximum normalized midspan displacement and the time instant $t_{\max}$ at which it occurs are affected by the fractional derivative order. In particular, the maximum displacement does not occur at the time instant $t_{\rm m} = 0.5L/V_F$ in which the moving load reaches the midspan section. For the limiting value $\alpha = 0.00$, the fractional derivative term in the equation of motion represents a restoring force and the beam undergoes undamped vibrations. It can be observed that, as the fractional derivative order increases, the time-history of midspan displacement exhibits less oscillations [29]. Similar results are obtained for a larger moving load velocity i.e., $V_F = 20$ m/s, as shown in Fig. 7.

The influence of the fractional derivative coefficient, c_α, is displayed in Fig. 8 for $\alpha = 0.25$. It can be observed that, when larger fractional derivative coefficients are considered, the amplitude of beam vibrations decreases and the time instant at which the maximum displacement occurs increases.

The influence of nonlinearities can be inferred from Fig. 9 which shows the comparison between the time-histories of beam normalized midspan displacement obtained retaining and neglecting the nonlinear term in the equation of motion for two different values of the fractional derivative order, $\alpha = 0.25$ and $\alpha = 0.50$. The linear and nonlinear solutions are also contrasted in Fig. 10 where the deformed configurations of the beam at the time instant $t_{\rm m} = 0.5L/V_F$ in which the moving load reaches the midspan section are plotted. It is noted that the proposed procedure is able to capture the appreciable deviation from the linear solution.

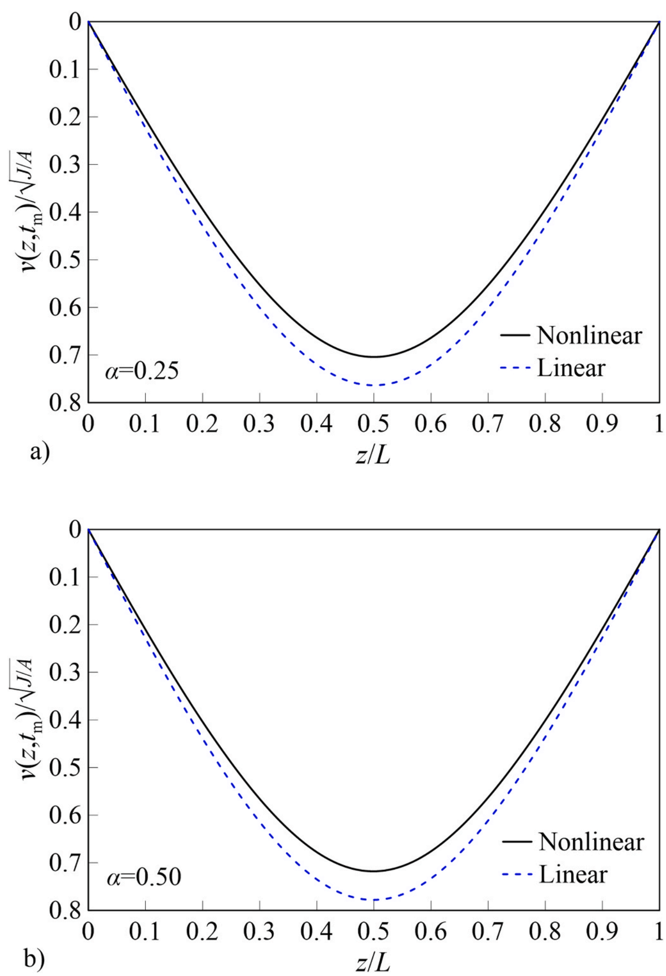

Fig. 10. Deformed configuration of the beam at the time instant t_m in which the moving load reaches the midspan section obtained retaining and neglecting nonlinearities: a) $\alpha = 0.25$; b) $\alpha = 0.50$ ($V_F = 10$ m/s).

5. Conclusions

The determination of the time-domain response of nonlinear beams endowed with a fractional derivative element crossed by moving loads has been addressed. Within the framework of a Galerkin-type solution procedure, beam transversal displacement has been represented as the superposition of linear modes of vibration with time-dependent amplitudes. A novel step-by-step scheme, labeled *improved pseudo-force method* (*IPFM*), has been developed for the numerical integration of the set of coupled nonlinear fractional differential equations governing the time-dependent modal amplitudes. The *IPFM* relies on the use of the Grünwald–Letnikov (*GL*) approximation of the fractional derivative. The key idea of the method is to treat terms depending on the unknown values of the response at the current time step as *pseudo-forces*. Such terms result from the nonlinear restoring forces as well as from the *GL* approximation of the fractional derivative which involves all past values of the response at discrete time instants. Nonlinearities are handled by performing iterations at each time step.

The proposed procedure can be applied to determine the time-domain response of nonlinear beams endowed with fractional derivative elements subjected to arbitrary dynamic excitations. A notable feature of the *IPFM* is that the matrices involved in the step-by-step integration scheme need to be computed only once since they depend on the time step size. Furthermore, unlike the classical Newmark-β method, the *IPFM* does not require the evaluation of the tangent stiffness matrix at each time step. The computational effort can be significantly reduced by performing a suitable truncation of the *GL* approximation of the fractional derivative i.e., retaining at each time step only terms associated with the most recent time-history.

The accuracy of the *IPFM* has been assessed by comparison with Newmark-β method. An excellent agreement between the two methods has been found for various values of the fractional derivative order. Numerical results have demonstrated that the time-domain response of the nonlinear beam under moving loads is significantly affected by the order and coefficient of the fractional derivative.

Author contributions

Alba Sofi: Conceptualization, Methodology, Software, Validation, Visualization, Original draft preparation, Writing- Reviewing and Editing.

Declaration of competing interest

The authors declare that they have no known competing financial interests or personal relationships that could have appeared to influence the work reported in this paper.

Data availability

Data will be made available on request.

APPENDIX A. Newmark-β method

The set of coupled nonlinear fractional differential equations governing the generalized time-dependent coordinates of the beam (Eq. (12)) can be written in the following incremental form [47]:

$$\Delta\ddot{\mathbf{q}}_{n+1} + \mathbf{\Omega}^2\,\Delta\mathbf{q}_{n+1} + \frac{c_\alpha}{\rho A}\left[{}_0^{GL}\mathscr{D}_t^\alpha\langle\mathbf{q}(t_{n+1})\rangle - {}_0^{GL}\mathscr{D}_t^\alpha\langle\mathbf{q}(t_n)\rangle\right] + \Delta\mathbf{p}_{\mathrm{NL},n+1}(\mathbf{q}(t_n),\mathbf{q}(t_{n+1})) = \Delta\mathbf{f}_{\mathrm{v},n+1} \quad \text{(A.1)}$$

where

$$\begin{aligned}&\Delta\mathbf{q}_{n+1} = \mathbf{q}(t_{n+1}) - \mathbf{q}(t_n);\\ &\Delta\ddot{\mathbf{q}}_{n+1} = \ddot{\mathbf{q}}(t_{n+1}) - \ddot{\mathbf{q}}(t_n);\\ &\Delta\mathbf{p}_{\mathrm{NL},n+1}(\mathbf{q}(t_n),\mathbf{q}(t_{n+1})) = \mathbf{p}_{\mathrm{NL}}(\mathbf{q}(t_{n+1})) - \mathbf{p}_{\mathrm{NL}}(\mathbf{q}(t_n));\\ &\Delta\mathbf{f}_{\mathrm{v},n+1} = \mathbf{f}_{\mathrm{v}}(t_{n+1}) - \mathbf{f}_{\mathrm{v}}(t_n).\end{aligned} \quad \text{(A.2a-d)}$$

Furthermore, by applying the *GL* approximation (Eq. (5)), the third term on the left-hand side of Eq. (A.1) can be expressed as:

$$\frac{c_\alpha}{\rho A}\left[{}_0^{GL}\mathscr{D}_t^\alpha\langle\mathbf{q}(t_{n+1})\rangle - {}_0^{GL}\mathscr{D}_t^\alpha\langle\mathbf{q}(t_n)\rangle\right] = \frac{c_\alpha}{\rho A}\frac{1}{(\Delta t)^\alpha}\left[\lambda_1(\alpha)\Delta\mathbf{q}_{n+1} + \sum_{j=2}^{n}\lambda_j(\alpha)\Delta\mathbf{q}_{n-j+2} + \lambda_{n+1}(\alpha)\mathbf{q}(t_1)\right]. \quad \text{(A.3)}$$

The increment of the nonlinear restoring forces can be approximated in terms of the tangent stiffness matrix $\mathbf{K}_{\mathrm{T},n}$ at the beginning of the time step:

$$\Delta \mathbf{p}_{\mathrm{NL},n+1}(\mathbf{q}(t_n),\mathbf{q}(t_{n+1})) \simeq \left.\frac{\partial \mathbf{p}_{\mathrm{NL}}(\mathbf{q})}{\partial \mathbf{q}}\right|_{t=t_n} \Delta \mathbf{q}_{n+1} = \mathbf{K}_{\mathrm{T},n}\Delta \mathbf{q}_{n+1}. \tag{A.4}$$

Taking into account the definition of the nonlinear restoring forces $\mathbf{p}_{\mathrm{NL}}(\mathbf{q}(t))$ in Eq. (13), the tangent stiffness matrix takes the following form:

$$\mathbf{K}_{\mathrm{T},n} = \left.\frac{\partial \mathbf{p}_{\mathrm{NL}}(\mathbf{q})}{\partial \mathbf{q}}\right|_{t=t_n} = -\frac{EA}{2L}\left[2\mathbf{R}\mathbf{q}(t_n)\mathbf{q}^{\mathrm{T}}(t_n)\mathbf{S} + \mathbf{q}^{\mathrm{T}}(t_n)\mathbf{S}\mathbf{q}(t_n)\mathbf{R}\right]. \tag{A.5}$$

Substituting Eqs. (A.3) and (A.4), and rearranging terms, Eq. (A.1) can be recast as:

$$\Delta \ddot{\mathbf{q}}_{n+1} + \mathbf{\Omega}^2\,\Delta \mathbf{q}_{n+1} + \frac{c_\alpha}{\rho A}\frac{1}{(\Delta t)^\alpha}\lambda_1(\alpha)\Delta \mathbf{q}_{n+1} + \mathbf{K}_{\mathrm{T},n}\Delta \mathbf{q}_{n+1} = \Delta \mathbf{f}_{\mathrm{v},n+1} - \frac{c_\alpha}{\rho A}\frac{1}{(\Delta t)^\alpha}\left[\sum_{j=2}^{n}\lambda_j(\alpha)\Delta \mathbf{q}_{n-j+2} + \lambda_{n+1}(\alpha)\mathbf{q}(t_1)\right]. \tag{A.6}$$

The Newmark $-\beta$ method is based on the following relationships:

$$\mathbf{q}(t_{n+1}) = \mathbf{q}(t_n) + \Delta t\dot{\mathbf{q}}(t_n) + \frac{\Delta t^2}{2}\left[(1-2\beta)\ddot{\mathbf{q}}(t_n) + 2\beta\ddot{\mathbf{q}}(t_{n+1})\right] \tag{A.7a}$$

$$\dot{\mathbf{q}}(t_{n+1}) = \dot{\mathbf{q}}(t_n) + \Delta t\left[(1-\gamma)\ddot{\mathbf{q}}(t_n) + \gamma\ddot{\mathbf{q}}(t_{n+1})\right] \tag{A.7b}$$

where the parameters β and γ define the variation of acceleration over a time step and determine stability and accuracy characteristics of the method. As known, $\gamma = 1/2$ and $\beta = 1/4$ correspond to the assumption of constant average acceleration which leads to an unconditionally stable integration scheme; $\gamma = 1/2$ and $\beta = 1/6$ correspond to the assumption of linear variation of acceleration.

By simple mathematical manipulations, Eqs. (A.7a,b) yield the following expressions:

$$\Delta \ddot{\mathbf{q}}_{n+1} = \frac{\Delta \mathbf{q}_{n+1}}{\beta \Delta t^2} - \frac{\dot{\mathbf{q}}(t_n)}{\beta \Delta t} - \frac{\ddot{\mathbf{q}}(t_n)}{2\beta} \tag{A.8a}$$

$$\Delta \dot{\mathbf{q}}_{n+1} = \frac{\gamma}{\beta \Delta t}\Delta \mathbf{q}_{n+1} - \frac{\gamma}{\beta}\dot{\mathbf{q}}(t_n) + \Delta t\left(1 - \frac{\gamma}{2\beta}\right)\ddot{\mathbf{q}}(t_n). \tag{A.8b}$$

Replacing Eq. (A.8a) into Eq. (A.6), the following relationship is obtained:

$$\mathbf{K}_{\mathrm{eff},n}\Delta \mathbf{q}_{n+1} = \mathbf{P}_{\mathrm{eff},n} \tag{A.9}$$

where

$$\mathbf{K}_{\mathrm{eff},n} = \mathbf{\Omega}^2 + \left[\frac{c_\alpha}{\rho A}\frac{\lambda_1(\alpha)}{(\Delta t)^\alpha} + \frac{1}{\beta \Delta t^2}\right]\mathbf{I}_{n_b} + \mathbf{K}_{\mathrm{T},n} \tag{A.10}$$

and

$$\mathbf{P}_{\mathrm{eff},n} = \Delta \mathbf{f}_{\mathrm{v},n+1} - \frac{c_\alpha}{\rho A}\frac{1}{(\Delta t)^\alpha}\left[\sum_{j=2}^{n}\lambda_j(\alpha)\Delta \mathbf{q}_{n-j+2} + \lambda_{n+1}(\alpha)\mathbf{q}(t_1)\right] + \frac{1}{\beta \Delta t}\dot{\mathbf{q}}(t_n) + \frac{1}{2\beta}\ddot{\mathbf{q}}(t_n). \tag{A.11}$$

By solving Eq. (A.9), the increment $\Delta \mathbf{q}_{n+1}$ is obtained:

$$\Delta \mathbf{q}_{n+1} = \left(\mathbf{K}_{\mathrm{eff},n}\right)^{-1}\mathbf{P}_{\mathrm{eff},n}. \tag{A.12}$$

Substituting Eq. (A.12) into Eqs. (A.8a,b), the increments of $\Delta \dot{\mathbf{q}}_{n+1}$ and $\Delta \ddot{\mathbf{q}}_{n+1}$ can be derived. Then, the solution at the time step t_{n+1} can be evaluated as:

$$\mathbf{q}(t_{n+1}) = \mathbf{q}(t_n) + \Delta \mathbf{q}_{n+1}; \tag{A.13a}$$

$$\dot{\mathbf{q}}(t_{n+1}) = \dot{\mathbf{q}}(t_n) + \Delta \dot{\mathbf{q}}_{n+1}. \tag{A.13b}$$

The acceleration at the end of the time interval, $\ddot{\mathbf{q}}(t_{n+1})$, can be computed from the equation of motion at the time instant t_{n+1} to guarantee dynamic equilibrium (see Eq. (12)), i.e.:

$$\ddot{\mathbf{q}}(t_{n+1}) = -\mathbf{\Omega}^2\,\mathbf{q}(t_{n+1}) - \frac{c_\alpha}{\rho A}\,{}_0^C\mathscr{D}_t^\alpha\langle \mathbf{q}(t_{n+1})\rangle - \mathbf{p}_{\mathrm{NL}}(\mathbf{q}(t_{n+1})) + \mathbf{f}_{\mathrm{v}}(t_{n+1}) \tag{A.14}$$

where the fractional derivative term can be expressed by using the *GL* approximation in Eq. (5).

Newton-Raphson iterations can be readily incorporated into the above-described incremental procedure.

References

[1] I. Podlubny, Fractional Differential Equations. An Introduction to Fractional Derivatives, Fractional Differential Equations, to Methods of Their Solution and Some of Their Applications, Academic Press, San Diego, CA, 1998.

[2] G.S. Samko, A.A. Kilbas, O.I. Marichev, Fractional Integrals and Derivatives, Gordon and Breach Science Publishers, Amsterdam, 1993.

[3] T.M. Atanackovic, S. Pilipovic, B. Stankovic, D. Zorica, Fractional Calculus with Applications in Mechanics: Wave Propagation, Impact and Variational Principles, John Wiley & Sons, 2014.

[4] F. Mainardi, Fractional Calculus and Waves in Linear Viscoelasticity: an Introduction to Mathematical Models, second ed., World Scientific, 2022 https://doi.org/10.1142/p926.
[5] A. Carpinteri, F. Mainardi, Fractals and Fractional Calculus in Continuum Mechanics, Springer Verlag, 1997.
[6] J. Sabatier, O.P. Agrawal, J.A. Tenreiro Machado, Advances in Fractional Calculus: Theoretical Developments and Applications in Physics and Engineering, Springer Netherlands, Dordrecht, The Netherlands, 2007.
[7] P.G. Nutting, A new general law deformation, J. Franklin Inst. 191 (1921) 679–685, https://doi.org/10.1016/S0016-0032(21)90171-6.
[8] A. Gemant, On fractional differentials, London, Edinburgh Dublin Phil. Mag. J. Sci. 25 (1938) 540–549, https://doi.org/10.1080/14786443808562036.
[9] M. Di Paola, A. Pirrotta, A. Valenza, Visco-elastic behavior through fractional calculus: an easier method for best fitting experimental results, Mech. Mater. 43 (12) (2011) 799–806, https://doi.org/10.1016/j.mechmat.2011.08.016.
[10] R.L. Bagley, P.J. Torvik, A theoretical basis for the application of fractional calculus to viscoelasticity, J. Rheol. 27 (1983) 201–210, https://doi.org/10.1122/1.549724.
[11] R.L. Bagley, P.J. Torvik, Fractional calculus—a different approach to the analysis of viscoelastically damped structures, AIAA J. 21 (1983) 741–748, https://doi.org/10.2514/3.8142.
[12] R.L. Bagley, P.J. Torvik, Fractional calculus in the transient analysis of viscoelastically damped structures, AIAA J. 23 (1985) 918–925, https://doi.org/10.2514/3.9007.
[13] Y.A. Rossikhin, M.V. Shitikova, Applications of fractional calculus to dynamic problems of linear and nonlinear hereditary mechanics of solids, Appl. Mech. Rev. 50 (1997) 15, https://doi.org/10.1115/1.3101682.
[14] Y.A. Rossikhin, M.V. Shitikova, Application of fractional calculus for dynamic problems of solid mechanics: novel trends and recent results, Appl. Mech. Rev. 63 (2010), 010801, https://doi.org/10.1115/1.4000563.
[15] M.V. Shitikova, Fractional operator viscoelastic models in dynamic problems of mechanics of solids: a review, Mech. Solid. 57 (2022) 1–33, https://doi.org/10.3103/S0025654422010022.
[16] M. Di Paola, R. Heuer, A. Pirrotta, Fractional visco-elastic Euler–Bernoulli beam, Int. J. Solid Struct. 50 (2013) 3505–3510, https://doi.org/10.1016/j.ijsolstr.2013.06.010.
[17] A. Pirrotta, S. Cutrona, S. Di Lorenzo, A. Di Matteo, Fractional visco-elastic Timoshenko beam deflection via single equation, Int. J. Numer. Methods Eng. 104 (2015) 869–886, https://doi.org/10.1002/nme.4956.
[18] Z. Zhu, G. Li, C. Cheng, Quasi-static and dynamical analysis for viscoelastic Timoshenko beam with fractional derivative constitutive relation, Appl. Math. Mech. 23 (2002) 1–12, https://doi.org/10.1007/BF02437724.
[19] R. Lewandowski, P. Wielentejczyk, Nonlinear vibration of viscoelastic beams described using fractional order derivatives, J. Sound Vib. 399 (2017) 228–243, https://doi.org/10.1016/j.jsv.2017.03.032.
[20] R. Lewandowski, Nonlinear steady state vibrations of beams made of the fractional Zener material using an exponential version of the harmonic balance method, Meccanica 57 (2022) 2337–2354, https://doi.org/10.1007/s11012-022-01576-8.
[21] G. Zhang, Z. Wu, Y. Li, Nonlinear dynamic analysis of fractional damped viscoelastic beams, Int. J. Struct. Stabil. Dynam. 19 (2019), https://doi.org/10.1142/S0219455419501293. Article number 1950129.
[22] K.B. Liaskos, A.A. Pantelous, I.A. Kougioumtzoglou, A.T. Meimaris, A. Pirrotta, Implicit analytic solutions for a nonlinear fractional partial differential beam equation, Commun. Nonlinear Sci. Numer. Simul. 85 (2020), 105219, https://doi.org/10.1016/j.cnsns.2020.105219.
[23] M. Javadi, M. Rahmanian, Nonlinear vibration of fractional Kelvin–Voigt viscoelastic beam on nonlinear elastic foundation, Commun. Nonlinear Sci. Numer. Simul. 98 (2021), https://doi.org/10.1016/j.cnsns.2021.105784.
[24] O.P. Agrawal, Analytical solution for stochastic response of a fractionally damped beam, J. Vib. Acoust., Trans. ASME 126 (4) (2004) 561–566, https://doi.org/10.1115/1.1805003, 2004.
[25] K.B. Liaskos, A.A. Pantelous, I.A. Kougioumtzoglou, A.T. Meimaris, Implicit analytic solutions for the linear stochastic partial differential beam equation with fractional derivative terms, Syst. Control Lett. 121 (2018) 38–49, https://doi.org/10.1016/j.sysconle.2018.09.001.
[26] P.D. Spanos, G. Malara, Nonlinear random vibrations of beams with fractional derivative elements, J. Eng. Mech. 140 (9) (2014), 04014069, https://doi.org/10.1061/(ASCE)EM.1943-7889.0000778.
[27] P.D. Spanos, G. Malara, Nonlinear vibrations of beams and plates with fractional derivative elements subject to combined harmonic and random excitations, Probabilist. Eng. Mech. 59 (2020), 103043, https://doi.org/10.1016/j.probengmech.2020.103043.
[28] Y. Jiao, W. Xu, Y. Song, Nonlinear response of beams with viscoelastic elements by an iterative linearization method, Int. J. Non Lin. Mech. 146 (2022), 104132, https://doi.org/10.1016/j.ijnonlinmec.2022.104132.
[29] R. Abu-Mallouh, I. Abu-Alshaikha, H.S. Zibdeh, Khaled Ramadan, Response of fractionally damped beams with general boundary conditions subjected to moving loads, Shock Vib. 19 (2012) 333–347, https://doi.org/10.3233/SAV-2010-0634.
[30] J. Freundlich, Dynamic response of a simply supported viscoelastic beam of a fractional derivative type to a moving force load, J. Theor. Appl. Mech. 54 (4) (2016) 1433–1445, https://doi.org/10.15632/jtam-pl.54.4.1433, 2016.
[31] R.K. Praharaj, N. Datta, Dynamic response of Euler–Bernoulli beam resting on fractionally damped viscoelastic foundation subjected to a moving point load, Proc IMechE Part C: J. Mech. Eng. Sci. 234 (24) (2020) 1–12, https://doi.org/10.1177/09544062209325.
[32] I. Podlubny, Matrix approach to discrete fractional calculus, Fract. Calc. Appl. Anal. 3 (4) (2000) 359–386.
[33] R.K. Praharaj, N. Datta, Dynamic response spectra of fractionally damped viscoelastic beams subjected to moving load, Mech. Base. Des. Struct. Mach. 50 (2) (2022) 672–686, https://doi.org/10.1080/15397734.2020.1725563.
[34] L.M. Anague Tabejieu, B.R. Nana Nbendjo, P. Woafo, On the dynamics of Rayleigh beams resting on fractional-order viscoelastic Pasternak foundations subjected to moving loads, Chaos, Solitons Fractals 93 (2016) 39–47, https://doi.org/10.1016/j.chaos.2016.10.001.
[35] A. Ouzizi, F. Abdoun, L. Azrar, Nonlinear dynamics of beams on nonlinear fractional viscoelastic foundation subjected to moving load with variable speed, J. Sound Vib. 523 (2022), 116730, https://doi.org/10.1016/j.jsv.2021.116730.
[36] J. Padovan, Computational algorithms for FE formulations involving fractional operators, Comput, Mech 2 (1987) 271–287, https://doi.org/10.1007/BF00296422.
[37] A. Schmidt, L. Gaul, On the numerical evaluation of fractional derivatives in multi-degree-of-freedom systems, Signal Process. 86 (2006) 2592–2601, https://doi.org/10.1016/j.sigpro.2006.02.006.
[38] R. Scherer, S.L. Kalla, Y. Tang, J. Huangc, The Grünwald–Letnikov method for fractional differential equations, Comput. Math. Appl. 62 (2011) 902–917, https://doi.org/10.1016/j.camwa.2011.03.054.
[39] P.D. Spanos, G.I. Evangelatos, Response of a non-linear system with restoring forces governed by fractional derivatives—time domain simulation and statistical linearization solution, Soil Dynam. Earthq. Eng. 30 (2010) 811–821, https://doi.org/10.1016/j.soildyn.2010.01.013.
[40] M.P. Singh, T.-S. Chang, H. Nandan, Algorithms for seismic analysis of MDOF systems with fractional derivatives, Eng. Struct. 33 (8) (2011) 2371–2381, https://doi.org/10.1016/j.engstruct.2011.04.010.
[41] J. Xu, J. Li, Stochastic dynamic response and reliability assessment of controlled structures with fractional derivative model of viscoelastic dampers, Mech. Syst. Signal Process. 72–73 (2016) 865–896, https://doi.org/10.1016/j.ymssp.2015.11.016.
[42] A. Sofi, G. Muscolino, Improved pseudo-force approach for Monte Carlo Simulation of non-linear fractional oscillators under stochastic excitation, Probabilist. Eng. Mech. 71 (2023), 103403, https://doi.org/10.1016/j.probengmech.2022.103403.
[43] G. Muscolino, Dynamically modified linear structures: deterministic and stochastic response, J. Eng. Mech. 122 (11) (1996) 1044–1051, https://doi.org/10.1061/(ASCE)0733-9399(1996)122:11(1044).
[44] A. D'Aveni, G. Muscolino, Response of non-classically damped structures in the modal subspace, Earthq. Eng. Struct. Dynam. 24 (1995) 1267–1281, https://doi.org/10.1002/eqe.4290240907.
[45] G. Borino, G. Muscolino, Mode-superposition methods in dynamic analysis of classically and non-classically damped linear systems, Earthq. Eng. Struct. Dynam. 14 (5) (1986) 705–717, https://doi.org/10.1002/eqe.4290140503.
[46] K.B. Oldham, J. Spanier, The fractional calculus, in: Mathematics in Science and Engineering vol. 111, Academic Press, New York, 1974.
[47] R.W. Clough, J. Penzien, Dynamics of Structurs, McGraw-Hill, New York, 1975.